



## Project Summary

# Dosimetry for *In-Vitro* Chick Brain Calcium-Ion Efflux Experiments by Numerical Methods Based on Zonal Harmonic Expansions

Guillermo Gonzalez and James C. Nearing

The full report discusses the calculation of the electric field and power density distribution in chick brain tissue inside a test tube, using an off-center spherical model. The off-center spherical model overcomes many of the limitations of the concentric spherical model and permits a more realistic modeling of the brain tissue as it sits in the bottom of the test tube surrounded by buffer solution. The effect of the unequal amount of buffer solution above the upper and below the lower surface of the brain is evaluated.

The field distribution is obtained in terms of a rapidly converging series of zonal harmonics. A method that permits the expansion of spherical harmonics about an off-center origin in terms of spherical harmonics at the origin is developed to calculate in closed form the electric field distribution.

Numerical results are presented for the adsorbed power density distribution and scaling ratios at carrier frequencies of 50 MHz, 100 MHz, and 147 MHz. It is shown that the off-center spherical model yields scaling ratios in the brain tissue that lie between the extreme values predicted by the concentric and isolated spherical models.

*This Project Summary was developed by EPA's Health Effects Research Laboratory, Research Triangle Park, NC, to announce key findings of the research project that is fully documented in a*

*separate report of the same title (see Project Report ordering information at back).*

### Introduction

A problem of considerable importance to the understanding of biological phenomena produced by electromagnetic radiation is the mechanism of interaction of amplitude-modulated radio-frequency [RF] waves on calcium-ion efflux from *in vitro* chick brain. Experiments have shown that when amplitude is modulated with extremely low frequency [ELF] sinusoidal waves, RF radiation can enhance the calcium-ion efflux from *in vitro* chick brain tissue.

In order to better understand the effects of amplitude-modulated RF radiation on calcium-ion efflux, the electromagnetic fields and absorbed power density distribution in the chick brain must be accurately determined. Concentric spherical models have been used to calculate the field and power density distribution in the chick brain. These models have provided much valuable information about the dosimetric aspects of the calcium-ion efflux experiments. The models have also been used to develop scaling ratios to determine the required incident power density that produces calcium-ion efflux at other carrier frequencies.

This study overcomes the limitations of the concentric spherical models. Concen-

tric spherical models do not adequately represent the chick brain half immersed in the buffer medium, because the brain as it sits in the bottom of the test tube is surrounded by a layer of buffer solution with a thickness that differs above and below the brain. Concentric spherical models use a uniform layer of buffer solution to surround the brain. To determine the dosimetric effects of the non-uniform layer, an off-center spherical model is used to approximate the physical geometry of the brain/buffer combination. The off-center spherical model represents a significant refinement to the concentric spherical model, since the brain can be modeled as a continuous, smooth, spherical surface surrounded by unequal amounts of buffer solution on its upper and lower surfaces. The electric field and absorbed power density distributions, and scaling ratios for carrier waves of 50, 100, and 147 MHz are calculated using a quasi-static approximation. This approximation leads to a field representation in terms of a convergent series involving spherical harmonics.

### Procedure

The schematic of the experimental set-up is shown in Figure 1. The chick brain tissue sits at the bottom of the test tube and is surrounded by a non-uniform layer of buffer solution.

The analytical model for the off-center spherical model of the brain inside a test tube is shown in Figure 2, along with the direction of the incident electric field. This model represents the geometry in Figure 1. In fact, except for the flat-topped buffer region, the model is reasonably accurate. The radii  $a$  and  $b$ , and the off center distance  $d$ , are selected so that the brain volume occupies 0.3 ml, and the buffer volume, 1 ml. Also, the limiting case as  $h$  approaches zero is analyzed.

The mathematical formulation that follows is by no means a simple extension of the concentric spherical case. To the best of the authors' knowledge, exact solutions to off-center spherical geometries of the type shown in Figure 2 in terms of zonal harmonic expansions have not appeared in the literature.

The mathematical formulation of the problem follows. The electric field, assuming quasi-static conditions, can be expressed as

$$\underline{E} = -\nabla\phi$$

where  $\phi$  is the electrostatic potential. The quasi-static approximation is valid be-

cause of the dimensions, frequencies, and electrical properties of the materials involved. In our calculations, the relative complex permittivity of the brain tissue at the typical carrier frequencies used in

calcium-ion studies are 100-j175 at 50 MHz, 72-j94.9 at 100 MHz, and 66-j69.2 at 147 MHz; for the buffer, the values are 71-j580 at 50 MHz, 71-j290 at 100 MHz, and 71-j200 at 147 MHz.

The externally applied field, which makes an angle of  $90^\circ$  with the  $z$ -axis (i.e.,  $\underline{E} = E_0 u_y$ ), produces a potential which can be expressed in spherical coordinates in the form

$$V_{\text{ext}} = -E_0 r_a Y_{11}^0(\theta_a, \phi)$$

or

$$V_{\text{ext}} = -E_0 r_b Y_{11}^0(\theta_b, \phi)$$

where

$$Y_{nm}^0(\theta, \phi) = \cos m\phi P_n^m(\cos\theta)$$

$P_n^m(\cos\theta)$  are associated Legendre polynomials.

The potential in regions I, II, and III satisfies Poisson's equation, subject to the appropriate boundary conditions. The charge distributions at  $r_a = a$  and  $r_b = b$  produce potentials  $V_a$  and  $V_b$  of the form

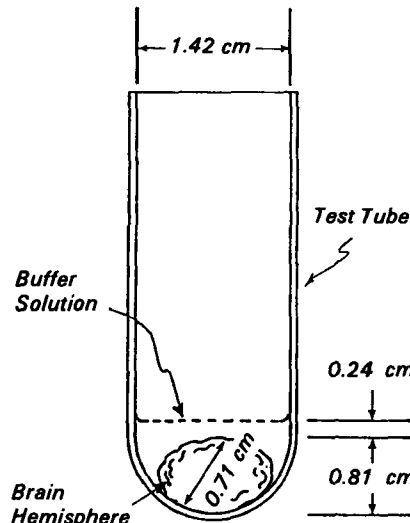


Figure 1. Schematic of the chick brain inside a test tube containing a buffer solution.

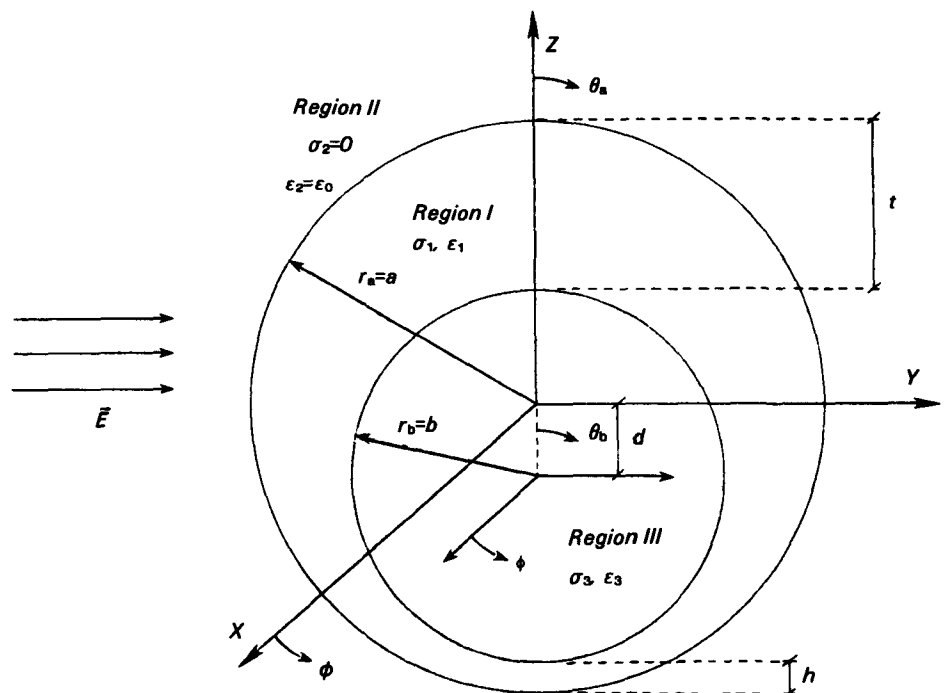


Figure 2. Off center spherical model for the chick brain.

$$V_a = \begin{cases} V_{a, in} = \sum_{n=0}^{\infty} \sum_{m=0}^n \alpha_{nm} \left(\frac{r_a}{a}\right)^n Y_{nm}^e(\theta_a, \phi) & (r_a \leq a) \\ V_{a, out} = \sum_{n=0}^{\infty} \sum_{m=0}^n \alpha_{nm} \left(\frac{a}{r_a}\right)^{n+1} Y_{nm}^e(\theta_a, \phi) & (r_a \geq a) \end{cases} \quad (1)$$

and

$$V_b = \begin{cases} V_{b, in} = \sum_{n=0}^{\infty} \sum_{m=0}^n \beta_{nm} \left(\frac{r_b}{b}\right)^n Y_{nm}^e(\theta_b, \phi) & (r_b \leq b) \\ V_{b, out} = \sum_{n=0}^{\infty} \sum_{m=0}^n \beta_{nm} \left(\frac{b}{r_b}\right)^{n+1} Y_{nm}^e(\theta_b, \phi) & (r_b \geq b) \end{cases} \quad (2)$$

where  $\alpha_{nm}$  and  $\beta_{nm}$  are constants to be determined from the boundary conditions. In terms of (1) and (2), the potentials in the three regions are given by

$$V_I = V_{a, in} + V_{b, out} + V_{ext} \quad (3)$$

$$V_{II} = V_{a, out} + V_{b, out} + V_{ext} \quad (4)$$

$$V_{III} = V_{a, in} + V_{b, in} + V_{ext} \quad (5)$$

The form selected for the potentials in (1) and (2) satisfy the continuity conditions at  $r_a = a$  and  $r_b = b$ . Therefore, the boundary conditions that remain to be satisfied at the interface are the continuity of the normal component of the current density at  $r_a = a$  and  $r_b = b$ .

In order to apply the boundary conditions at the surface of the off-center sphere (i.e., at  $r_b = b$ ), we need to expand the solution  $V_{a, in}$  in terms of the coordinates  $r_b, \theta_b$  and  $\phi$ , and the solution  $V_{b, out}$  in terms of the coordinates  $r_a, \theta_a$ , and  $\phi$ . The necessary expansions are

$$V_{a, in} = \sum_{n=0}^{\infty} \sum_{m=0}^n \alpha_{nm} a^{-n} \sum_{s=m}^n f_{snm} r_b^s Y_{sm}^e(\theta_b, \phi) \quad (6)$$

and

$$V_{b, out} = \sum_{n=0}^{\infty} \sum_{m=0}^n \beta_{nm} b^{n+1} \sum_{s=m}^n g_{snm} r_a^{-s-1} Y_{sm}^e(\theta_a, \phi) \quad (7)$$

where

$$f_{snm} = \frac{(-1)^{n-s} (n+m)! d^{n-s}}{(n-s)! (s+m)!}$$

and

$$g_{snm} = \frac{d^{s-n} (s-m)!}{(n-m)! (s-n)!}$$

Applying the boundary conditions to (3), (4), and (5), and using (6) and (7), a set of linear equations for the  $n=j$  ( $j=0,1,\dots$ ) and  $m=k$  ( $k=0,1,\dots,n$ ) coefficients (i.e.,  $\alpha_{jk}$  and  $\beta_{jk}$ ) are obtained.

Fixing the maximum  $n$  to be  $N_{max}$ , the set of linear equations is solved for  $\alpha_{jk}$  and  $\beta_{jk}$ . The results are then inserted into (1) to (5) to calculate the potential, electric field, and absorbed power density distribution in the three regions.

## Results and Discussion

The absorbed power density distributions, assuming  $E_0=1$  V/m, were calculated for several cases; the most important was for a brain volume of  $0.3$  cm<sup>3</sup>, buffer volume of  $1$  cm<sup>3</sup>, and  $h=0.05$  cm. Therefore,  $a=0.677$  cm,  $b=0.415$  cm,  $d=0.212$  cm, and  $t=0.474$  cm. Also, the limiting cases as  $h$  and  $d$  approach zero are considered. For  $h \rightarrow 0$  (i.e., when the spheres touch at the bottom) the dimensions are  $a=0.677$  cm,  $b=0.415$  cm,  $d=0.262$  cm, and  $t=0.524$  cm.

Figures 3 and 4 graphically illustrate the absorbed power density distribution produced by an incident carrier wave, with  $E_0=1$  V/m, at  $147$  MHz for the cases where  $h=0.05$  cm and  $d \rightarrow 0$ , respectively. In the figures, each line represents a constant absorbed power density level. The

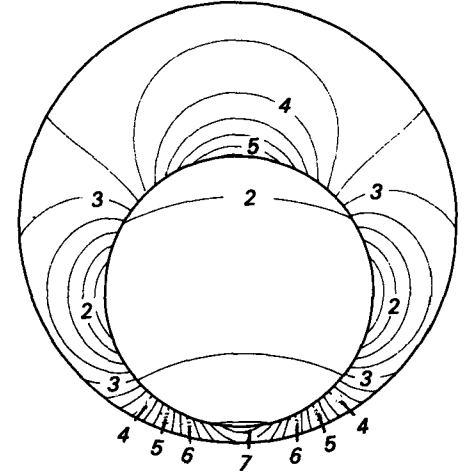


Figure 3. Absorbed power density distribution at  $147$  MHz. The dimensions are  $a=0.677$  cm,  $b=0.415$  cm,  $d=0.212$  cm,  $h=0.05$  cm and  $t=0.474$  cm. The number scale (0 to 9) is linear, where 9 represents an absorbed power density of  $0.5$  mW/m<sup>3</sup> for an incident field of  $E_0=1$  V/m.

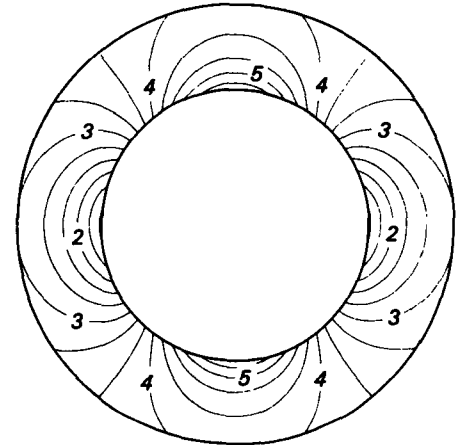


Figure 4. Absorbed power density distribution at  $147$  MHz for a centered spherical model ( $d=0$ ). The dimensions are  $a=0.677$  cm,  $b=0.415$  cm, and  $t=h=0.262$  cm. The number scale (0 to 9) is linear, where 9 represents an absorbed power density of  $0.5$  mW/m<sup>3</sup> for an incident field of  $E_0=1$  V/m.

number scale is linear, ranging from 0 to 9, where 9 represents an absorbed power density of  $0.5$  mW/m<sup>3</sup>. For example, the value of 2 represents an absorbed power density of  $(2/9)0.5=0.111$  mW/m<sup>3</sup>. In

Figure 4, the absorbed power density distribution in the brain region is constant at a value of  $0.109 \text{ mW/m}^3$ .

Absorbed power density patterns similar to those shown in Figures 3 and 4 are produced at 50 and 100 MHz, except that the absorbed power levels are smaller.

It is significant to observe from Figure 3 that the absorbed power density distribution in the brain region is not uniform; the bottom of the chick brain has a higher absorbed power density than the top. Also, in Figures 3 and 4, the surface fields around the chick brain exhibit a significant variation from the bottom to the top.

Scaling relations were calculated for the off-center spherical model. Figure 5 gives the values of the scaling factor,  $P_i(50)/P_i(147)$ , for points along the z-axis inside the spherical brain between the top (i.e.,  $z=0.415 \text{ cm}$ ) and bottom (i.e.,  $z=-0.415 \text{ cm}$ ). Figure 6 gives the values of the scaling factors for points on the outside surface of the brain between the top (i.e.,  $\theta=0$ ) and bottom (i.e.,  $\theta=\pi$ ) from  $0 \leq \theta \leq \pi$ . The scaling ratios at a given frequency are continuous at the top and bottom of the brain-buffer interface. This follows from the fact that the electric field is tangential and continuous at the top and bottom brain-buffer interface.

## Conclusions and Recommendations

The off-center spherical model was used to calculate the electric field and absorbed power density distribution in chick brain tissue inside a test tube. The calculations were made with typical dielectric data used in previous analytical studies for carrier frequencies of 50 MHz, 100 MHz, and 147 MHz. In the experimentally realistic case where the chick brain is surrounded by lesser amounts of buffer solution at the bottom, the pattern of absorbed power densities showed a marked concentration of absorbed power near the bottom. The absorbed power density within the brain showed only gradual variations with position. Outside, at the surface of the brain, the absorbed power density distribution varied by factors of 6 to 10.

The scaling ratios were calculated as a function of position for points inside, and on the outside surface of the brain. The off-center spherical model revealed that the scaling ratio inside the brain tissue is not constant; the maximum change ( $h=0$  case) from the top of the brain to the bottom was approximately 11% for  $P_i(50)/P_i(100)$ , and 19% for  $P_i(50)/P_i(147)$ . This contrasts with the concentric spherical

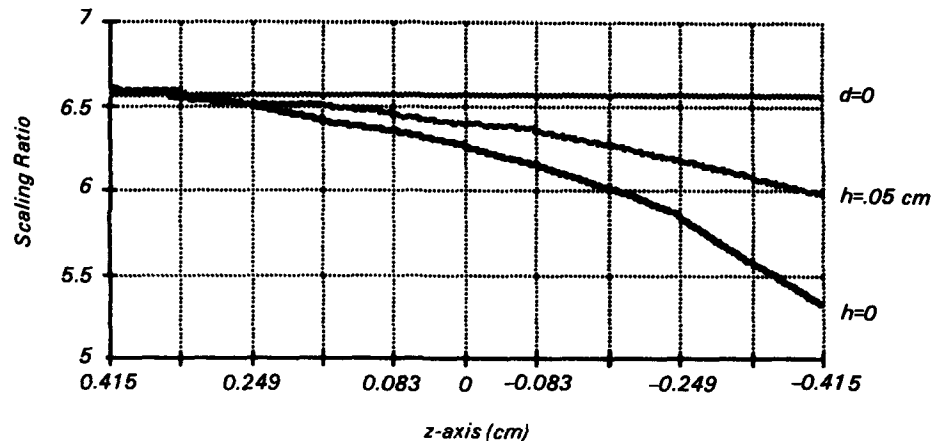


Figure 5. Scaling ratio values for  $P_i(50)/P_i(147)$  along the z-axis of the brain.

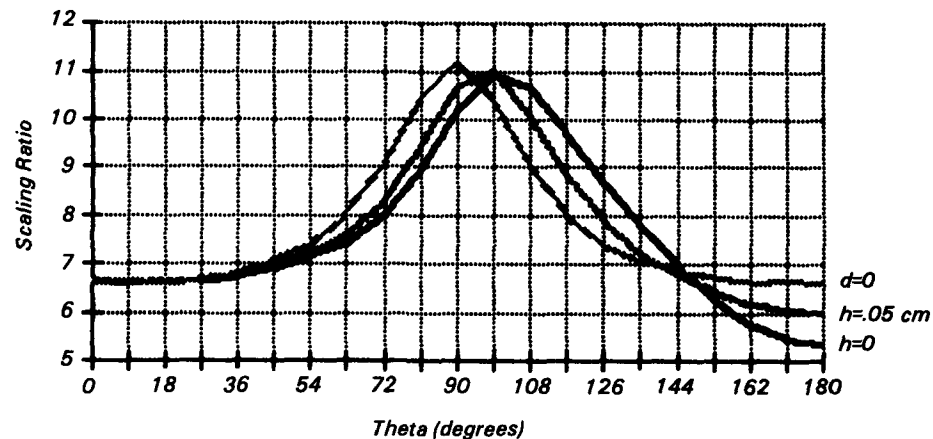


Figure 6. Scaling ratio values for  $P_i(50)/P_i(147)$  along the outside surface of the brain as a function of  $\theta$ .

model, which predicts no change. As expected, the scaling ratios near the top are essentially identical to the values predicted by the concentric spherical model; at the bottom, the values become closer to those predicted by an isolated spherical model. Thus, the off-center spherical model yields internal scaling ratios that lie between the extreme values predicted by the concentric and isolated spherical models.

Recent experimental studies have shown that the penetration of radioactive calcium-ions in chick brain tissue was no greater than 1 mm from the surface. Thus, it may be concluded that surface field values are of paramount importance. The profiles for the surface scaling ratios are symmetric for the concentric spheri-

cal case, with the peak value occurring at a point on the surface ( $\theta=90^\circ$ ), where the external electric field is normal to the surface. However, the off-center spherical model yielded somewhat lower peak values whose position shifted toward the bottom ( $\theta \approx 99^\circ$ ). In addition, the surface ratios were similar at the top of the brain for all the models, but the values at the bottom varied considerably, with the  $h=0$  case approaching the value given for an isolated sphere.

The scaling ratio results have provided new insights into the interpretation of the calcium-ion efflux phenomena. The experimentalists can use the information presented in this study to interpret their results and to formulate theories about calcium-ion efflux phenomena.

*Guillermo Gonzalez and James C. Nearing are with University of Miami, Coral Gables, FL 33124.*

*Ronald J. Spiegel is the EPA Project Officer (see below).*

*The complete report, entitled "Dosimetry for In-Vitro Chick Brain Calcium-Ion Efflux Experiments by Numerical Methods Based on Zonal Harmonic Expansions," (Order No. PB 85-227 528/AS; Cost: \$8.50, subject to change) will be available only from:*

*National Technical Information Service*

*5285 Port Royal Road*

*Springfield, VA 22161*

*Telephone: 703-487-4650*

*The EPA Project Officer can be contacted at:*

*Health Effects Research Laboratory*

*U.S. Environmental Protection Agency*

*Research Triangle Park, NC 27711*

United States  
Environmental Protection  
Agency

Center for Environmental Research  
Information  
Cincinnati OH 45268

Official Business  
Penalty for Private Use \$300

EPA/600/S1-85/016

0000329 PS

U S ENVIR PROTECTION AGENCY  
REGION 5 LIBRARY  
230 S DEARBORN STREET  
CHICAGO IL 60604